NOISE AND ENTROPY IN NON-EQUIPARTITIONED PARTICLE BEAMS

I. Hofmann and O. Boine-Frankenheim
GSI Helmholtzzentrum für Schwerionenforschung GmbH, Planckstr.1, 64291 Darmstadt, Germany
Technische Universität Darmstadt, Schlossgartenstr.8, 64289 Darmstadt, Germany

Abstract

The numerical noise inherent to particle-in-cell (PIC) simulation of 3d high intensity bunched beams in periodic focusing is explored on the basis of the rms entropy model by Struckmeier and of simulations with the TRACEWIN code using linac relevant parameters. Starting from noise in a matched equilibrium beam and its dependence on grid and particle number we explore the relevance of this noise under dynamical situations. The cases under study are fast emittance exchange; an initially mismatched beam; slow crossing through space charge structure resonances. We find that an effect of the equilibrium noise can be retrieved in a dynamical case, if the process is evolving sufficiently slowly.

INTRODUCTION

In this paper we deal with the numerical noise generated by the discreteness of the spatial grid used for the Poisson solver as well as the effect of artificial collisions due to using highly charged super-particles. In simulation of extended plasmas this type of noise received attention since the 1970's, when interest in this field was growing in parallel with the performance of numerical computation.

More recently, the interest has revived to get a quantitative understanding of this noise in the field of high intensity beam simulation, where numerical noise may play a role for long-term simulation. In this context new interest was found in the analytical modelling of noise and the associated entropy growth based on the rms entropy model by Struckmeier [1, 2]. It is based on second order moments of the Vlasov-Fokker-Planck equation and assumes that collisional behaviour and temperature anisotropy can drive rms emittance growth, which is used to define an rms entropy growth. The associated noise and entropy growth in 2d beams - the transverse 4d phase space - is studied in a recent paper by Boine-Frankenheim et al. [3]. A companion paper by Hofmann et al. [4] deals with the rms entropy model and noise in 3d short bunches - in 6d phase space - with particular emphasis on linear accelerator applications. Some results of the latter are reviewed in the following section.

REVIEW OF ENTROPY AND NOISE THEORY

The basic equation for the rms entropy growth is based on the idea that the change of the six-dimensional rms emittance defined as product of individual plane rms emittances, $\epsilon_{6d} \equiv \epsilon_x \epsilon_y \epsilon_z$, is a suitable measure for rms entropy growth, hence the system noise. The resulting relative change of rms emittance is given by:

$$\frac{1}{k}\Delta S = \frac{\Delta \epsilon_{6d}}{\epsilon_{6d}} = \Delta s \frac{k_f^\star}{3} \; (I_A + I_{GN}) \tag{1}$$

with a term related to temperature anisotropy,

$$I_A \equiv \left(\frac{(T_x - T_y)^2}{T_{xy}} + \frac{(T_x - T_z)^2}{T_{xz}} + \frac{(T_y - T_z)^2}{T_{yz}} \right), \tag{2}$$

$k^\star$ the dynamical friction coefficient and I_{GN} describing an offset explained as grid noise in connection with the periodic focusing (see Ref. [4]).

We consider a periodic FODO lattice of 1000 cells with symmetrically arranged rf kicks. The zero current phase advance per cell of this lattice is assumed to be $k_0 = 60°$ in x, y, z with equal emittances in all three directions. The beam is matched for a Gaussian distribution and the current is chosen such that the tune depression is $k/k_0 \approx 0.55$. The envelopes obtained with the TRACEWIN code are shown in Fig. 1:

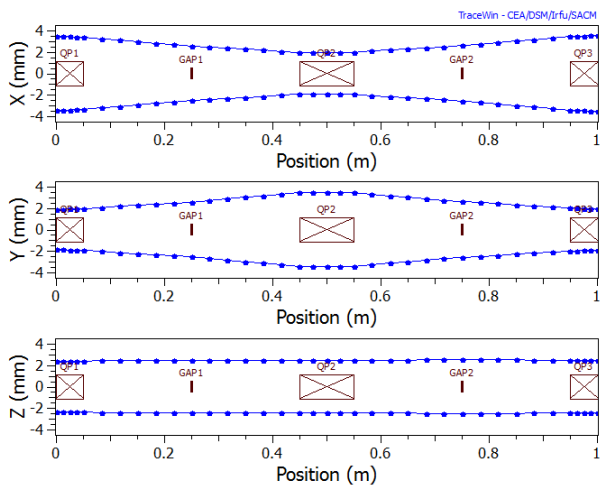

Figure 1: Basic cell of periodical FODO lattice with rf gaps.

The alternating focusing causes a strong modulation and local imbalance of "temperatures". According to Eq. 2, with more details in Ref. [1], this purely collisional effect is as source of entropy growth, which is amplified by grid heating effects Ref. [4]. Following Ref. [4], results for the relative growth of ϵ_{6d} are shown in Fig. 2 as function of n_c and for different N. The $n_{cx,y,z}$ are understood as half number of cells between the maximum grid extent values of $\pm 3.5\sigma$. Beyond, the mesh is replaced by an analytical continuation for the space charge potential based on a Gaussian core of identical rms size. We note that the number of space charge

ISBN 978-3-95450-173-1

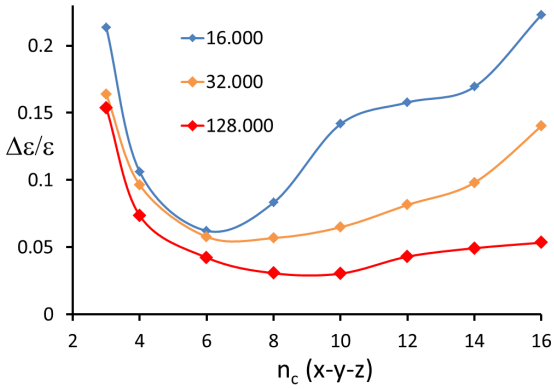

Figure 2: Relative growth of ϵ_{6d} in FODO lattice of Fig. 1 for N=16.000/32.000/128.000, as function of the number of grid cells in x, y, z.

steps per lattice cell has been chosen here as 15 (10/m in TRACEWIN). Also, the option "linear interpolation" (on the grid) is chosen.

Note that $n_c = 7$ implies only two grid points per 1σ of the Gaussian profile. This can explain the steeply rising noise or "grid heating" for less resolution, with only small differences between numbers of particles. All three cases show that an *optimum value of* n_c exists, where the noise is minimum. It is the higher the larger N. The increase of $\Delta\epsilon_{6d}/\epsilon_{6d}$ above the optimum n_c is most pronounced for the case N=16.000, where an estimate shows that the number of simulation particles per grid cell is only as low as approximately 1 for $n_c = 16$, which explains the strong rise of the noise. It is also seen that large N is efficient only if the grid resolution is sufficiently large. For N=128.000 the gentle increase of the noise when rising above $n_c = 10$ might be indicative of an increase of the Coulomb logarithm with higher resolution of the colliding charges.

In summary, for $N \approx 10^5$ and a matched equilibrium beam at moderate space charge tune depression of about 50% an optimum $n_c \approx 8...10$ exists. In the following we explore to what extent the initial equilibrium noise level is relevant for describing dynamical situations driven by mismatch or resonances. This is obviously a complex discussion, and the following examples can only be a first attempt.

EMITTANCE EXCHANGE AND NOISE

In linear accelerators it is understood that collision effects between real particles play no role, and emittance exchange can only occur due to resonant processes. For our discussion of simulation beams and the understanding of noise, it is nonetheless of interest to first explore the role of grid and collision noise in a case of anisotropy, but unaffected by resonances.

Grid and Collision Noise

Anisotropy as source of emittance exchange can be studied by choosing initially different emittances. We consider a Gaussian distribution function, $N = 16.000$, and compare small and larger values of n_c. In the first example of Fig. 3 we assume $n_c = 10$. An initial anisotropy with

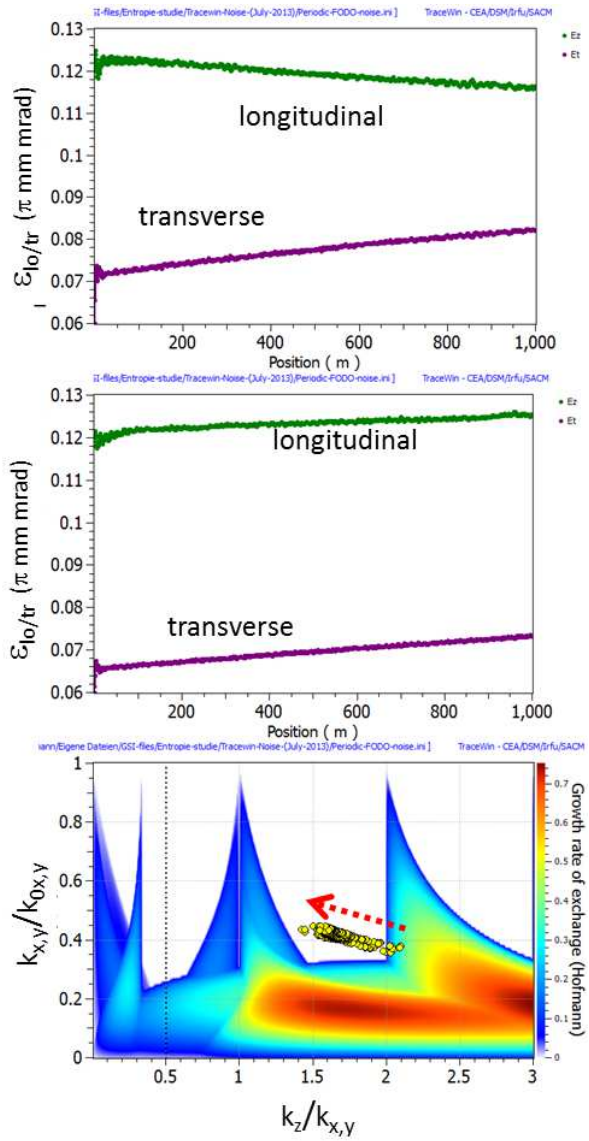

Figure 3: Rms emittances for $n_c = 10$ (top) and $n_c = 3$ (center); and stability chart (bottom, colour scale indicating theoretical rates of emittance change) for grid resolution $n_c = 10$.

$\epsilon_z/\epsilon_{x,y} = 2$ is assumed for zero current phase advances $k_{0x,y,z} = 52°/52°/60°$, with corresponding initial space charge depressed tunes of $k_{x,y,z} \approx 21°/21°/37°$. The slight splitting of zero current tunes between z and x, y is chosen in the example to avoid the resonant coherent emittance exchange by the $k_z/k_{x,y} \approx 1$ resonance. The pronounced collisional effect leads to a shrinking longitudinal emittance, while the transverse emittance (average of ϵ_x and ϵ_y) grows.

ISBN 978-3-95450-173-1

It is expected from collisional behaviour - and consistent with Eq. 1 that the different temperatures of the ensemble relax towards an equipartitioned equilibrium. Note that the footprint of tunes in the bottom chart of Fig. 3 is taken over the 1000 periodic cells and entirely in the resonance-free region (few points exceeding $k_z/k_{x,y} = 2$ are caused by jitter only). The dashed (red) arrow in this chart marks the time evolution along the lattice.

Following Fig. 2, the noise level for a poor grid resolution $n_c = 3$ is close to that for $n_c = 10$ - only about 30% higher. The corresponding result - with parameters otherwise identical with Fig. 3 - is shown in the bottom graph of Fig. 3. This case is dominated by grid heating to the effect that all emittances increase. The increment of ϵ_{6d} is about comparable. This indicates the different nature of noise from grid heating and collisional heating in particular for anisotropic beams.

Resonant Exchange and Noise

Here we take again $\epsilon_z/\epsilon_{x,y} = 2$, but remove the splitting of tunes and assume $k_{0x,y,z} = 60°/60°/60°$, with corresponding $k_{x,y,z} \approx 26°/26°/35°$. We first use the larger $N = 10^5$ to keep collisions at a low level and assume $n_c = 6$, which is close to the bottom noise level of Fig. 2. Results are shown in the top of Fig. 4. It is noted that a rapid partial emittance exchange occurs during less than the first 20 cells. It is caused by the $k_z/k_{x,y} = 1$ resonance, which is driven by the space charge octupole [5]. This process is so fast that a noise effect should not be expected. This is confirmed by a comparison with the same calculation carried out with N as low as 10^3 in the center of Fig. 4. In spite of the much stronger noise effect for $N = 10^3$ the fast resonant exchange is practically unchanged and thus not influenced by the noise. It is followed by a collisional emittance exchange until complete equipartition and, beyond this point, a continuing growth of both emittances.

INITIALLY MISMATCHED BEAMS

Here we refer to mismatch as one of the sources of halo formation and beam loss in high current linacs. In the following example we assume parameters (before mismatch) as for Fig. 2, with $N = 10^5$ and a large initial envelope mismatch by a factor $MM = 1.6$ in all planes. It is known that under the repeating action of mismatch oscillations particles are resonantly driven into a beam halo. In Fig. 5 we show the resulting 99.9% emittances in x, y, z (top) and ϵ_{6d} (center) for a case with $n_c = 6$, which indicates the rapid conversion of mismatch into a halo population within about 50 periods. As quantitative measure for the transport into the halo region we also plot the percentage of particles, which are detected outside a radius of 5 mm after period 1000 (MM=1.6 and MM=1.2/1.2/1.6), where this radius marks the beam edge (99.9% of particles) in the absence of mismatch (MM=1). The percentage of particles into halo is seen to be practically insensitive to the grid resolution - even for the strong grid heating case $n_c = 3$. This is not unexpected in view of the rapid halo formation process. The early behaviour of

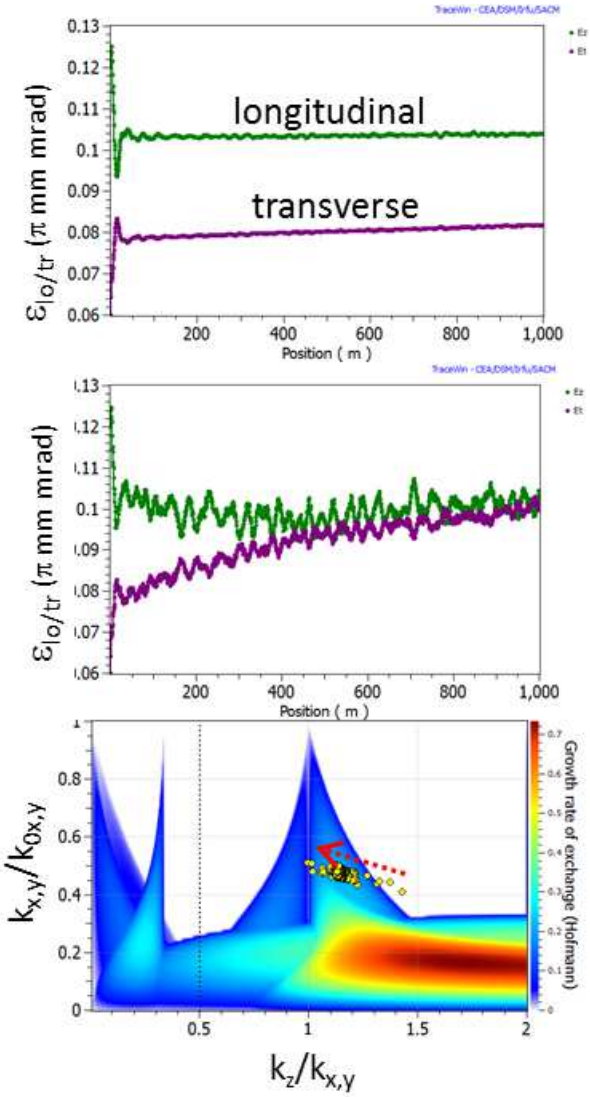

Figure 4: Resonant case: rms emittances for $N = 10^5$(top) and $N = 10^3$ (center); and stability chart (bottom, for $N = 10^5$).

ϵ_{6d} is dominated by the coherent mismatch oscillations and becomes noise- or entropy-like only after about 200 cells.

RESONANCE DRIVEN EMITTANCE GROWTH

In contrast with the preceding examples of "fast processes" we study here the behaviour for slow resonant processes by relatively slow crossing of low order resonances driven by space charge multipoles.

$90° \rightarrow 60°$ *Tune Scan*

For a beam as used in Fig. 2 and with $N = 10^5$ we now assume a tune scan from $k_{0x,y,z} = 90°/90°/60°$ to $k_{0x,y,z} = 60°/60°/60°$ over 500 cells between cell 100 and 600 as shown in Fig. 6. Note that this scan leads to a scan of the rms value $k_{x,y}$ from approximately $55° \rightarrow 35°$. We note

ISBN 978-3-95450-173-1

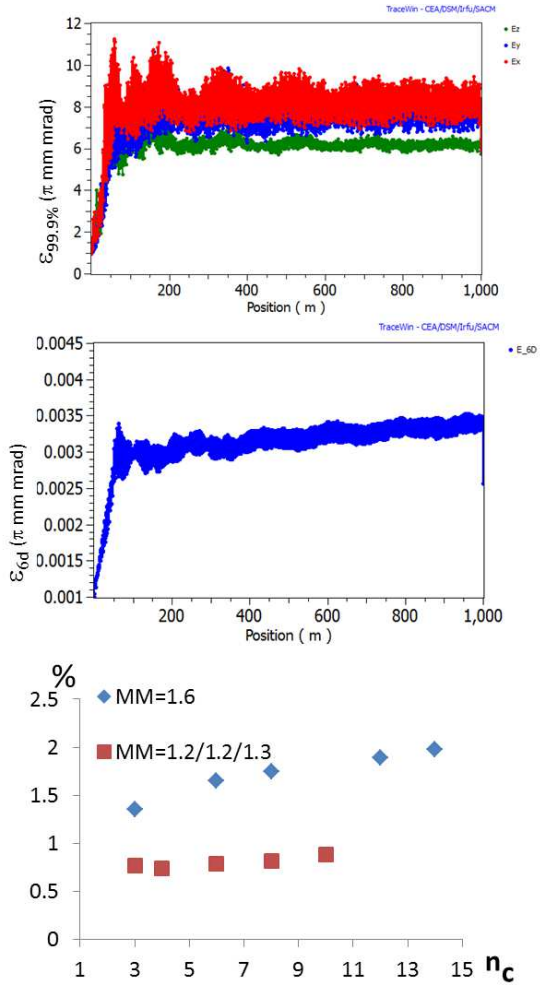

Figure 5: Mismatch action (MM=1.6) on $\epsilon_{99.9\%}$ (top), ϵ_{6d} (center) and percentage of particles into halo ($R > 5$ mm) as function of n_c (bottom).

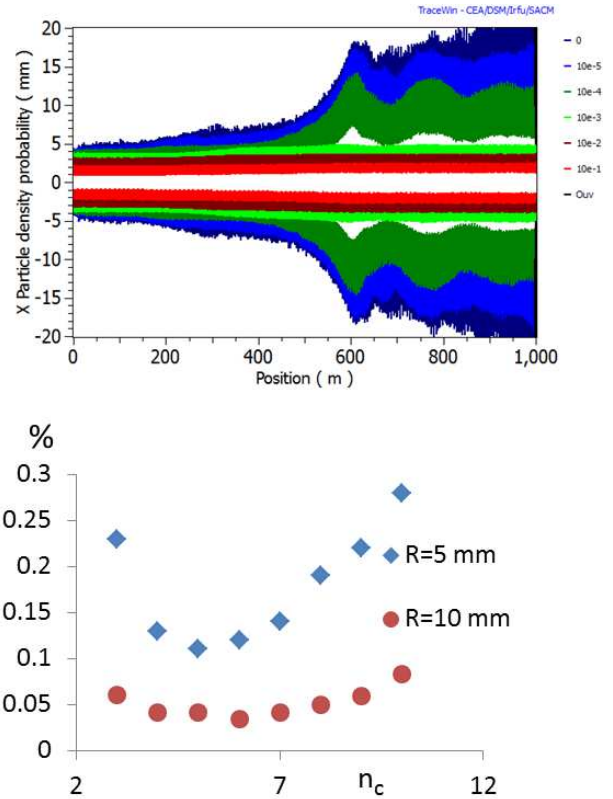

Figure 6: x-density probability (top) and percentage of particles into halo ($R > 5/10$ mm) as function of n_c (bottom), for $n_c = 7$.

that the rms value of $k_{x,y}$ is crossing the value 45° at about cell 300. This indicates the center of a resonant stopband due to $4 \times 45 = 180°$, possibly also $8 \times 45 = 360°$ (see also Ref. [6]), for which there is an indication in the density probability plot. In Fig. 6 we show the x-density probability as well as the halo percentage into $R = 5$ and $R = 10$ mm apertures.

Comparing with the case $N = 128.000$ in Fig. 2 we suggest that the grid heating regime for small n_c is reflected in the halo percentage. However, in the region $6 \leq n_c \leq 10$ the (collisional) noise is practically not increasing, while the halo percentage rises by almost a factor of 3 ($R = 5$ mm). This rise is nearly unchanged, if we increase N to 10^6.

This result seems to indicate that for a slowly occurring resonance crossing the constancy of the noise level in equilibrium - with regard to rising n_c - is not a guarantee that the percentage of particles into the halo is properly described by the simulation. Instead, it seems that a larger n_c and thus higher accuracy in space charge potential calculation gives a more reliable prediction of the halo population.

90° *Stop-Band Crossing*

A much stronger type of space charge resonance occurs in the vicinity of the 90° stop-band. The condition $4 \times 90 \approx 360°$ gives rise to resonance with the space charge pseudo-octupole as was shown experimentally [7], whereas theoretically also the so-called envelope instability (with $2 \times 90° \approx 180°$) might occur near this condition [6]. This crossing is realized in the simulation by a scan from $k_{0x} = 105° \rightarrow 88°$ during 1000 cells and fixed $k_{0y,z} = 105°/60°$ as shown in Fig. 7 for $N = 128.000$ and $n_c = 6$. The initial (rms) depressed tunes are $k_{x,y,z} = 91.5°/91.5°/49°$. The 4-th order resonance results in trapping of particles in four islands. This process becomes visible already after the first few cells and leads to their increasing separation from the core. Their separation as well as their rotation in the $x - x'$ phase are also identified in the x-density profile.

Increasing the grid resolution to $n_c = 12$ we have found, however, a significant deviation. There is no longer a void between core and islands, and more particles get extracted from the core. The $x - x'$ plot at 570 m actually indicates a strong presence of an envelope mode, which breaks the four-fold symmetry in the previous example. We attribute it to the envelope instability, which - surprisingly - was not found in the simulation with $n_c = 6$. The associated core oscillation is also visible in the x-density profile. We found that plotting $\epsilon_{x,53\%}$, the emittance of an ellipse including

ISBN 978-3-95450-173-1

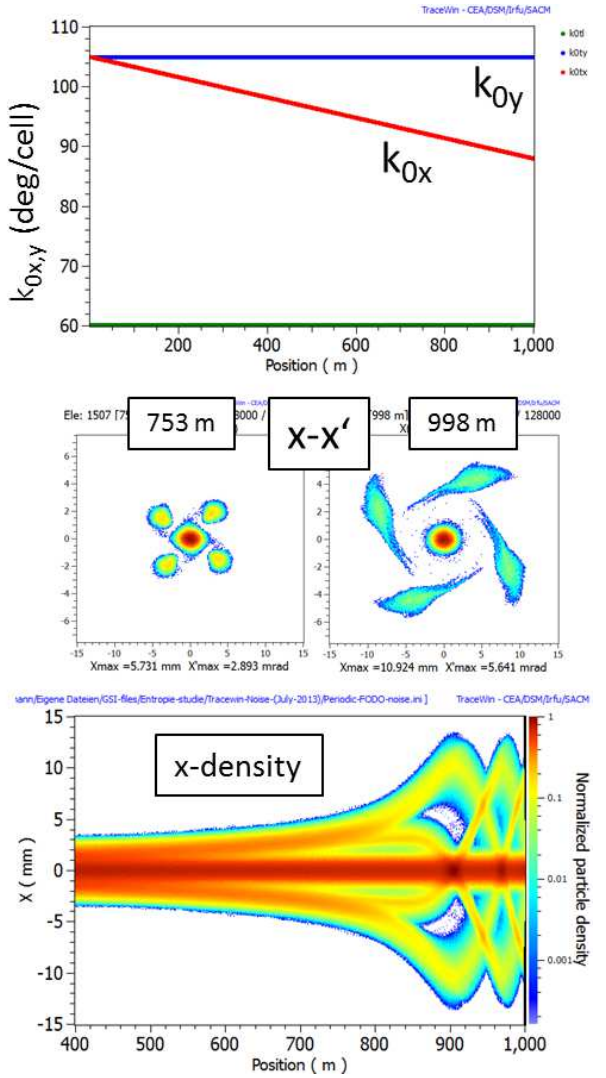

Figure 7: Tune scan (top), $x - x'$ phase space plots (center) and x-density profile (bottom) for $n_c = 6$.

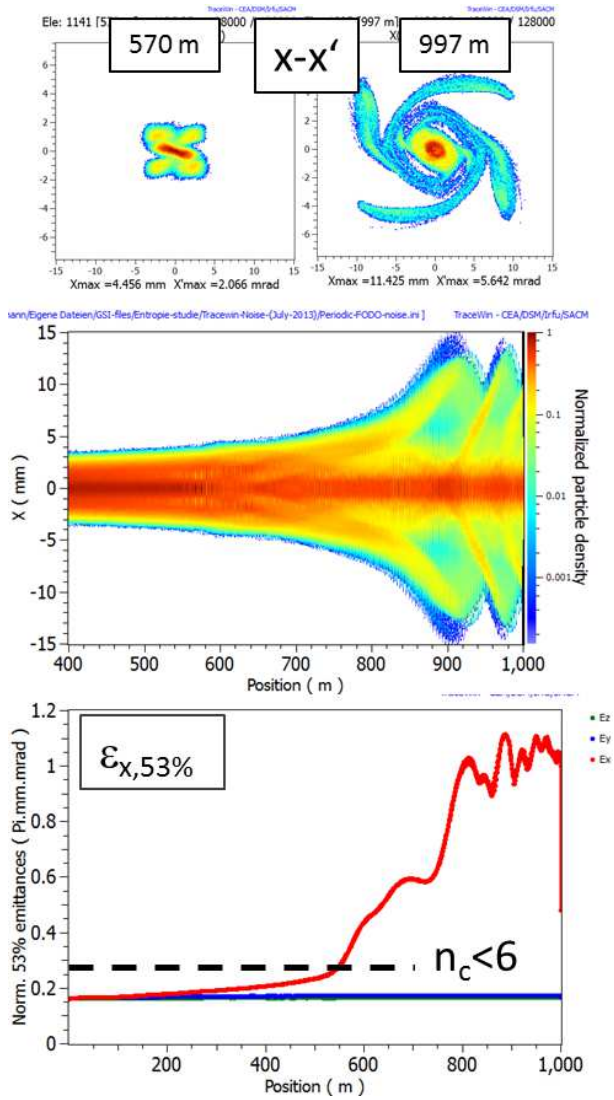

Figure 8: $x - x'$ phase space plots (top), x-density profile (center) and $\epsilon_{x,53\%}$ for $n_c = 12$.

53% of the particles, is a practical measure as it is chosen to include a fraction of particles trapped in the islands. Results as function of n_c and for different N are summarized in Fig. 9 in terms of the growth in $\epsilon_{x,53\%}$, including cases, which have been evaluated only until cell 600. The results indicate a "jump" in the behaviour for $n_c > 6$, independent of N. Apparently the additional feature occurs only subsequent to the development of the islands and thus becomes visible beyond approximately 600 cells. We cannot at present explain this behaviour as it is not obvious why a lower order resonance mode - the envelope mode - should appear only for higher n_c. A possible explanation might be the degradation of grid resolution in the core, while the grid cells grow with increasing distance of the islands from the center. Also, the envelope instability is growing exponentially from noise level - assuming an initially envelope matched beam - which makes this a noise sensitive process.

CONCLUSION

We have explored the validity of the 6d rms emittance concept as measure for beam entropy growth driven by grid *and* collision induced noise, in particular under dynamical conditions beyond equilibrium. We find that noise only matters for sufficiently slow processes - fast emittance exchange or mismatch evolution is insensitive to it. For slow resonances, on the other hand, the equilibrium noise optimum at moderate resolution is not necessarily sufficient. In our examples higher grid resolution appears advantageous to resolve complex higher order resonance behaviour. These examples justify more work to be done in order to develop practically useful guidelines.

ISBN 978-3-95450-173-1

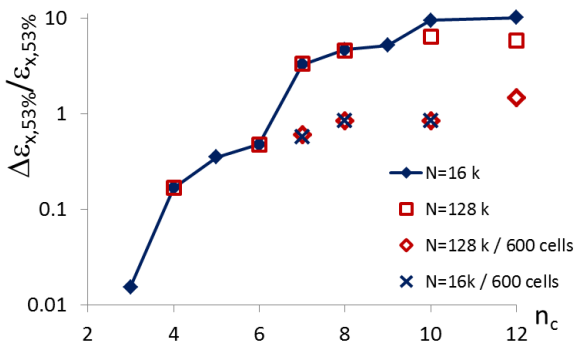

Figure 9: Comparison of maximum values of $\epsilon_{x,53\%}$ for different N as function of grid resolution.

REFERENCES

[1] J. Struckmeier, Phys. Rev. E 54, 830 (1996).

[2] J. Struckmeier, Phys. Rev. ST Accel. Beams 6, 034202 (2000).

[3] O. Boine-Frankenheim, I. Hofmann, J. Struckmeier and S. Appel, Nuclear Instruments and Methods in Physics Research A 770, 164 (2015.)

[4] I. Hofmann O. Boine-Frankenheim, to be published in Phys. Rev. ST Accel. Beams (2014).

[5] I. Hofmann, G. Franchetti, O. Boine-Frankenheim, J. Qiang, and R. D. Ryne, Phys. Rev. ST Accel. Beams 6, 024202 (2003).

[6] I. Hofmann, L.J. Laslett, L. Smith and I. Haber, *Part. Accel.* **13**, 145 (1983).

[7] L. Groening et al., Phys. Rev. Lett. **102**, 234801 (2009).

ISBN 978-3-95450-173-1